



Practical Jointed Approach to Functionally Graded Structures

Ibrahim KELES^{a*}, Kutay AYDIN^b

^a Department of Mechanical Engineering, Samsun University, Samsun 55000, Turkey

^b Department of Mechanical Engineering, Amasya University, Amasya 05100, Turkey

*E-mail address: ibrahim.keles@samsun.edu.tr^a, kutay.aydin@amasya.edu.tr^b

ORCID numbers of authors:

0000-0003-3614-4877^a 0000-0001-8252-2635^b

Received date: 04.05.2020

Accepted date: 10.07.2020

Abstract

In this study, a practical jointed approach in the forced vibration investigation of functionally graded material (FGM) structures under internal pressure are applied by modified Durbin's method. The FGM material consists of heterogeneous material that shows exponential variation in the thickness. Four types of dynamic loads are applied to the FGM cylinder for forced vibration. Displacement and stress distributions due to non-homogeneous constant are intended. Stress distribution dependent on the homogeneity parameter is computed and the results obtained for cylindrical structures were compared with the finite element method (FEM). The inhomogeneity parameter is empirically regulated, with a continuously changing volume fraction of the ingredients. The parameters for homogeneity were randomly selected to show displacement and stress distributions.

Keywords: Functionally graded materials, Structural elements, Boundary value problems, Modified Durbin's method

1. Introduction

The structural elements of the pressure vessels used in engineering areas such as aerospace and petroleum are important in engineering applications such as cylinder and sphere. As a result, the internal loads are one of the main problems of industrial structures. It may lead to stress gradient and / or cracked nuclei occurring in the stress distribution of the specified loads. By the analysis of the structures under the influence of the internal pressure, it facilitates the determination of the density of the points affected by the stress and the unsuitable stress distributions. Previous research has provided analytical resolutions for homogeneous isotropic and orthotropic structures. Tranter [1], Mirsky [2], Klosner and Dym [3], Ahmed [4], Ghosh [5] have pioneered their work in the cylinders, discs and spheres due to axial symmetry.

The functional graded materials (FGM) are more advanced structural materials in determining the material properties in the direction of the thickness in the solution of problems due to the composite materials interfaces. Güven [6] explained the mechanical stress distribution of the isotropic functional grade thick walled sphere under the influence of internal pressure.



Tutuncu and Ozturk [7] presented exact solutions in the form of stresses occurring in functionally graded pressure vessels. A study close to this work was also printed by Horgan and Chan [8]. Obata and Noda [9] submitted the studies of constant thermal stresses in order to understand the design of the functional graded thick-walled spheres and cylinders and the effects of the stresses. Tutuncu and Temel [10] functional-grade hollow cylinders have solved the displacements and stresses of the disc and spheres using an analytical method. Differential equations and systems obtained in the analysis of stress distributions are not easy to solve with analytical methods. In most cases, this is impossible. Therefore, numerical methods are applied in case of large equation systems, non-linearity and complex geometry. Therefore, it is a good option to select a numerical method to determine the stress distributions of FGM cylinders and spheres.

Loy et al. [11] and Pradhan et al. [12] includes the dynamic response of heterogeneous cylinders to the vibration of FGM cylindrical projectiles using the Rayleigh-Ritz method. Bayat et al. [13] presented a flexible solution for the analysis of rotating discs classified as functional in variable thickness by considering the material properties and the disc thickness profile as two power law distributions. Xiang et al. [14] presented two recursive algorithms to determine extrusion stresses between two adjacent layers in a multilayer cylinder exposed to internal and external pressure. The effects of transient waves in the FGM cylinder on stresses and displacements using the hybrid numerical method were investigated by Han et al. [15]. Assuming that FGM thick hollow cylinders are made from many bottom rollers, the finite element vibration analysis is handled by Shakeri et al. [16]. Ng et al. [17] examined the stabilization of FGM cylindrical projectiles under axial harmonic loading.

The main idea behind the modelling of FGM structural elements is to create subdivisions of material that are homogeneous in themselves with different properties as is the case with graded behavior. Although some analytical solutions (see, e.g., Keles [18]) for this type of the problem is available in the literature, they either are restricted to one inhomogeneity parameter for all material properties that is not the case in real or contain complex solutions such that usually it is necessary to solve for each parameter separately, which is not practical for parametric analysis. From a parametric analysis point of view, for this type of problems numerical solution is becoming essential. In this study, we present the application of modified Durbin's method (MDM) as a numerical method for stress and displacement solutions of FGM cylinders of variable thickness. As a material feature, the change in thickness of the modulus of elasticity ($E(r) = E_0 r^\beta$) is defined. The results were compared with FEM compared with the results. The non-homogeneous β values were used to indicate the distribution over the stress. The inhomogeneity constant β used in the study does not represent a specific material. Forced vibration analysis of structures under the influence of dynamic internal pressure changes over time through the residue theorem of Cauchy, one of the analytical solutions, is valid only for simple internal pressure loads. In this context, in order to test the accuracy of the numerical method, Keles [18] compared the solution with the literature. It is inevitable to use numerical transformation methods to determine displacement and stress distributions of structures under point, point, continuous and repulsive internal pressure. Durbin's numerical inverse Laplace transform method was chosen in this study. It is seen that this method has been applied successfully in vibration analysis for different structural elements in the literature (see for example, [19]). Laplace transformation of such loads will not be possible, especially if the internal pressure is given in point or point form. It has been found in the literature (see for example, [20, 21]) that vibration analysis is successfully applied with different methods and assumptions for the load types that are possible for Laplace transformation. In this case, Durbin's method will provide a fast and effective result. MDM is

an efficient solution procedure whose theoretical background is available in the literature [22, 23]. The method is also successfully applied in other structural mechanics problems such as those involving spherical shells [24], Timoshenko beam [25] and cylinders [26]. Dynamic behavior of cylindrical structures of different values of inhomogeneity parameter is presented. The numerical method described can be conveniently applied to FGM cylinders, discs and spherical structural members. A comparison was made with FEM (ANSYS) to determine the accuracy and effectiveness of the numerical method.

2. Basic Equation

The stress and displacement distribution in a thick-walled hollow cylinder will be considered as the inner radius a and the outer radius ka where k is a constant. The elasticity modulus and density vary throughout the thickness as $E(r) = E_0 r^\beta$ and $\rho(r) = \rho_0 r^\beta$, respectively. The subscripted terms in Table 1 that is (i) and (o) are the material properties of FGM thick-walled hollow cylinder.

Table 1. Material properties of the FGM thick-walled hollow cylinder.

E_0 (GPa)	206			ρ_0 (g/cm ³)	7.85		
β	r (m)	$\rho_i=1$	$\rho_o=2$	β	r (m)	$\rho_i=1$	$\rho_o=2$
$E(r)=E_0 r^\beta$	-5	206	6.437	$\rho(r)=\rho_0 r^\beta$	-5	7.85	0.2453
(GPa)	-2	206	51.5	(g/cm ³)	-2	7.85	1.9625
	0	206	206		0	7.85	7.85
	2	206	824		2	7.85	31.4
	5	206	6592		5	7.85	251.2

2.1. Basic Formulation of FGM Cylinders

Strain-displacement and basic equations considering the assumption of plane strain are [7]

$$\varepsilon_r = \frac{du}{dr}, \quad \varepsilon_\theta = \frac{u}{r}, \tag{1}$$

$$\sigma_r = C_{11}(r)\varepsilon_r + C_{12}(r)\varepsilon_\theta, \tag{2}$$

$$\sigma_\theta = C_{12}(r)\varepsilon_r + C_{11}(r)\varepsilon_\theta,$$

where, with ν_0 the Poisson's ratio,

$$C_{11}(r) = \left(\frac{E_0(1-\nu_0)}{(1+\nu_0)(1-2\nu_0)}\right)r^\beta$$

and

$$C_{12}(r) = \left(\frac{E_0\nu_0}{(1+\nu_0)(1-2\nu_0)}\right)r^\beta.$$

The only nontrivial equilibrium equation under assumptions can be inscribed in the following form [5],

$$\frac{\partial \sigma_r}{\partial r} + \frac{\sigma_r - \sigma_\theta}{r} = \rho_0 r^\beta \frac{\partial^2 u}{\partial t^2} \tag{3}$$

Using Eqs. (1) - (3), basic equation of radial displacement becomes

$$\frac{r^2 \partial^2 u}{\partial r^2} + r \frac{\partial u}{\partial r} m_1 + m_2 u = \frac{r^2}{c^2} \frac{\partial^2 u}{\partial t^2} \quad (4)$$

where $c^2 = \frac{E_0(1-\nu_0)}{\rho_0(1+\nu_0)(1-2\nu_0)}$, $m_1 = \beta + 1$, $m_2 = \frac{\nu_0 \beta}{(1-\nu_0)} - 1$

with boundary conditions in radial directions

$$\sigma_r|_{r=a} = -P \text{ and } \sigma_r|_{r=ka} = 0 \quad (5)$$

Converting the dimensionless variables

$$v = \frac{u}{a}, x = \frac{r}{a}, \tau = \frac{ct}{a} \quad (6)$$

reduces Eq. (4) in the form

$$\frac{\partial^2 v}{\partial x^2} + \frac{m_1}{x} \frac{dv}{dx} + \frac{m_2}{x^2} v = \frac{\partial^2 v}{\partial \tau^2} \quad (7)$$

and boundary conditions are as follows

$$\sigma_r|_{x=1} = -P(\tau) \quad \sigma_r|_{x=k} = 0 \quad (8)$$

with the primary conditions

$$v = 0 \text{ and } \frac{\partial v}{\partial \tau} = 0 \text{ when } \tau = 0 \quad \text{for } 1 \leq x \leq k \quad (9)$$

The general equation of displacement in Laplace space takes the following form:

$$\bar{v}(x, p) = \mathcal{L}[v(x, \tau)] = \int_0^\infty v(x, \tau) e^{-p\tau} d\tau \quad (10)$$

where p is the Laplace parameter. Eq. (7) is converted to Laplace space by applying initial conditions to obtain the following equation:

$$\frac{d^2 \bar{v}}{dx^2} + \frac{m_1}{x} \frac{d\bar{v}}{dx} + \left(\frac{m_2}{x^2} - p^2\right) \bar{v} = 0 \quad (11)$$

The final form of boundary conditions in Laplace space will take the form

$$\bar{\sigma}_r|_{x=1} = -\bar{P}(p) \quad \bar{\sigma}_r|_{x=k} = 0 \quad (12)$$

Solution of Eq. (11) Bessel function expression

$$\bar{v}(x, p) = x^\phi (C_1 I_n(px) + C_2 K_n(px)) \quad (13)$$

where I_n and K_n are Bessel functions of first and second kind, respectively, of order n with

$$\phi = -\frac{\beta}{2}, n = \sqrt{1 - \frac{v_0\beta}{1-v_0} + \frac{\beta^2}{4}}$$

The final solution of the final solution using the iteration formulas (e.g. see reference [27]) in Laplace space by obtaining C_1 and C_2 by applying the general equation obtained without dimension using boundary conditions is as follows;

$$\bar{v}(x, p) = -\frac{\bar{F}(p)}{c_{11}} x^\phi \frac{F(p)}{G(p)} \quad (14)$$

where

$$F(p) = [K_n(pk)S_1 + pkK_{n-1}(pk)]I_n(px) - [I_n(pk)S_1 - pkI_{n-1}(pk)]K_n(px) \quad (15)$$

and

$$G(p) = [K_n(pk)S_1 + pkK_{n-1}(pk)][I_n(p)S_1 - pI_{n-1}(p)] - [K_n(p)S_1 + pK_{n-1}(p)][I_n(pk)S_1 - pkI_{n-1}(pk)] \quad (16)$$

where $S_1 = (n - m - \phi)$ and $m = \frac{c_{12}(r)}{c_{11}(r)}$

For displacement distribution in the FGM cylinder subject to internal pressure, Eq. 14 in Laplace space must be converted to real time space.

3. Numerical Inversion of Solution by the Modified Durbin's Method (MDM)

The numerical solution of forced vibration analysis for the FGM cylinder was obtained for a set value of the Laplace parameter. For the conversion of results to time space, the modified Durbin method is used. The inverse Laplace transformation method that provides the conversion of Durbin to time space is expressed as [18, 28]:

The meaning $f(t)$ at time t_j is assumed by

$$f(t_j) \cong \frac{2Exp[aj\Delta t]}{T} \left[-\frac{1}{2} Re\{\bar{F}(a)\} + Re\left\{ \sum_{k=0}^{N-1} (\bar{F}(p_k)L_k) Exp\left[i\left(\frac{2\pi}{N}\right)jk\right] \right\} \right], (j=0,1,2,\dots N-1) \quad (17)$$

where $\bar{F}(p_k)$ is the Laplace transform of $f(t)$. The k th Laplace parameter is demarcated as $p_k = a + ik\frac{2\pi}{T}$. The number N is $N = \frac{T}{\Delta t}$ where T is the solution recess and Δt is the time raise. The choice of constant 'a' is done by transmission a value to aT . It is proposed that the value of aT be in the range 5 to 10. For the mathematical samples offered in this paper this value is taken as 6. Finally, the results are adapted by multiplying each term in the precis by Lanczos factor L_k as recommended in (e.g. see reference [29]).

$$L_k = \frac{Sin(\frac{k\pi}{N})}{(\frac{k\pi}{N})}, (L_0=1) \quad (18)$$

If the Laplace transform of the function $f(t)$ is not given in closed-form as in the case of point-by-point definition, the discrete values need first to be transformed into the Laplace domain as follows:

$$\bar{F}(p_k) = \Delta t \sum_{n=0}^{N-1} [f(t_n) e^{-at_n}] e^{-i \frac{2\pi nk}{N}} \quad (19)$$

For various pressures only the term $\bar{P}(p)$ is altered in the solution certain by Eq. (14).

4. Implementation Disc and Spherical Structures

The expressions given the preceding sections can readily be used for solutions of FGM annular disks in plane stress with the material constants in Eq. (2) redefined as

$$C_{11}(r) = \frac{E_0}{1+\nu_0^2} r^\beta, \quad C_{12}(r) = \frac{E_0 \nu_0}{1+\nu_0^2} r^\beta \quad (20)$$

As for FGM spheres structure; u is

$$\varepsilon_r = \frac{\partial u}{\partial r} \text{ and } \varepsilon_\theta = \varepsilon_\varphi = \frac{u}{r} \quad (21)$$

Expressions between stress-strain are

$$\begin{aligned} \sigma_r &= C_{11} \varepsilon_r + C_{12} \varepsilon_\theta + C_{12} \varepsilon_\varphi = C_{11}(r) \varepsilon_r + 2C_{12}(r) \varepsilon_\theta \\ \sigma_\theta = \sigma_\varphi &= C_{12} \varepsilon_r + C_{11} \varepsilon_\theta + C_{12} \varepsilon_\varphi = C_{12}(r) \varepsilon_r + (C_{12}(r) + C_{11}(r)) \varepsilon_\theta \end{aligned} \quad (22)$$

The radial displacement solution given for the FGM cylinder is still legal with the next constraints now redefined as

$$\phi = -\left(\frac{1+\beta}{2}\right), n = \sqrt{\phi^2 - 2\left(\frac{\nu_0 \beta}{1-\nu_0} - 1\right)}, m = \frac{C_{12}(r)}{C_{11}(r)}, S_1 = (n - 2m - \phi) \quad (23)$$

5. Results

Figures (1,6) show comparison of the methods and evolution of circumferential stress σ_θ and radial displacement v for $\nu = 0.3, k = 2.0$ and $\beta = -5.0, -2.0, 0.0, 2.0, 5.0$. The boundary conditions for stresses are assumed as $\bar{\sigma}_r|_{x=1} = -\bar{P}(p), \bar{\sigma}_r|_{x=k} = 0$. In accordance with the material and geometric properties used in the numerical method model, commercial (ANSYS) finite element code was compared and generated [29]. Due to the symmetry in the cylinder, four of the four geometries formed in the finite element model are considered. In the finite element model, an 8-axis axial symmetric rectangular element is used. For the modeling of the cylindrical structures FGM, each layer was applied with 20 layers having a fixed material property value.

Results obtained by Keles [18] are used for validation purposes, analytical. The comparing will be illustrated in the Tables 2-3. It can be observed from Tables, the results are in good agreement with the same results from Keles [18]. It is proven that upon a screening results

given in Tables 2-3, a substantial amount of accuracy and efficiency is achieved using the MDM method.

Table 2. Comparison of MDM results with Keles [18] for the radial displacements with different dynamic loads applied to the inner surface of the cylinder. ($\beta = 0.0, \omega = 1.0, \gamma = 1.0, k = 2.0$)

τ	$P_1(\tau) = P_0(1 - \text{Cos}(\omega\tau))$		$P_2(\tau) = P_0$		$P_3(\tau) = P_0(1 - e^{-\gamma\tau})$	
	$v C_{II} / P_0$		$v C_{II} / P_0$		$v C_{II} / P_0$	
	Keles [18]	MDM	Keles [18]	MDM	Keles [18]	MDM
0	0	0,000003	0	0,00001	0	0,000001
5	6,54644	6,54643	4,88701	4,88700	4,17045	4,17043
10	-2,11269	-2,11267	0,07458	0,07456	0,83551	0,83550
15	5,33630	5,33629	4,78081	4,78079	4,26004	4,26002
20	-0,66194	-0,66191	0,23675	0,23674	0,76713	0,76710
25	7,32722	7,32720	4,62315	4,62313	4,30325	4,30323
30	-0,91986	-0,91984	0,42225	0,42224	0,73963	0,73960
35	5,09853	5,09851	4,49282	4,49280	4,3124	4,31239
40	-1,80397	-1,80396	0,55301	0,55300	0,73936	0,73934
45	6,66612	6,66610	4,44839	4,44837	4,30764	4,30762
50	0,16580	0,16579	0,58978	0,58976	0,74312	0,74310

Table 3. Comparison of MDM results with Keles [18] for the hoop stresses with different dynamic loads applied to the inner surface of the cylinder. ($\beta = 0.0, \omega = 1.0, \gamma = 1.0, k = 2.0$)

τ	$P_1(\tau) = P_0(1 - \text{Cos}(\omega\tau))$		$P_2(\tau) = P_0$		$P_3(\tau) = P_0(1 - e^{-\gamma\tau})$	
	σ_r / P_0		σ_r / P_0		σ_r / P_0	
	Keles [18]	MDM	Keles [18]	MDM	Keles [18]	MDM
0	0	0,000003	-0,41145	-0,41142	0,00002	0,00001
5	5,09078	5,09076	3,60494	3,60491	3,01761	3,01760
10	-2,51242	-2,51241	-0,35857	-0,35855	0,26815	0,26812
15	3,655910	3,655909	3,51747	3,51743	3,08857	3,08855
20	-0,79378	-0,79373	-0,22501	-0,22500	0,21180	0,21179
25	6,03100	6,03099	3,38763	3,38761	3,12415	3,12413
30	-1,11281	-1,11280	-0,07223	-0,07220	0,18916	0,18914
35	3,39960	3,39959	3,28029	3,28028	3,13169	3,13166
40	-2,18586	-2,18582	0,03545	0,03543	0,18894	0,18893
45	5,29085	5,29083	3,24369	3,24367	3,12777	3,12776
50	0,12184	0,12182	0,06574	0,06572	0,19204	0,19202

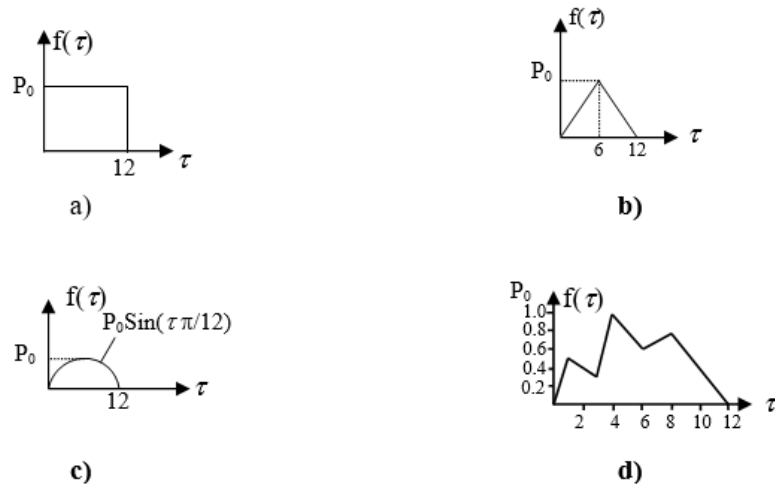


Fig. 1. Dynamic loads: (a) rectangular impulsive load, (b) triangular impulsive load, (c) half sinus impulsive load (d) impulsive load given discretely

In this study, results are offered for many impulsive deployed loads. Four cases of impulsive loadings (rectangular impulsive load, triangular impulsive load, half sinus impulsive load, impulsive load given discretely step) are considered (see Fig. 1). Figs. 2 and 3 show the effect of rectangular impulsive load on the radial displacements and circumferential stress of the suggested method and FEM. In Figs. 2 and 3, displacement decreases with increasing inhomogeneity parameter. Second, the triangular impulsive load is considered. Figs. 4 and 5 include displacements in the problem solved by the numerical method used and ANSYS software. As β increases, a decrease occurs in the value of circumferential stress in Figs. 4-5. When the numerical results of radial displacements and tangential stresses are compared with the results obtained with MDM and FEM, it is seen that the results are almost identical. Third, the half sinus impulsive load is considered. A collation of damping of radial displacement and stress are obtainable in Figs. 6-7. If the inhomogeneity constant is positive, it expresses the increase of hardness by providing stress protective effect in the radial direction. Finally, the impulsive load given discretely is considered. The radial displacements and circumferential stress of FG cylinder for inhomogeneity constant ($\beta = -5.0, -2.0, 0.0, 2.0, 5.0$) are presented in Figs. 8-9. It is clearly obvious that the radial displacements and circumferential stress for all approaches are identical (Figs. 8-9). It is seen that the results of Durbin's method solutions are overlapping with the model created using a commercial finite element code, FEM [30].

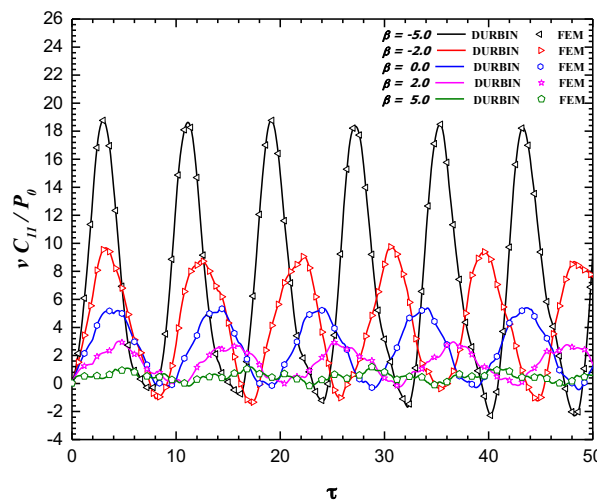


Fig. 2. Radial displacement versus time for rectangular impulsive load

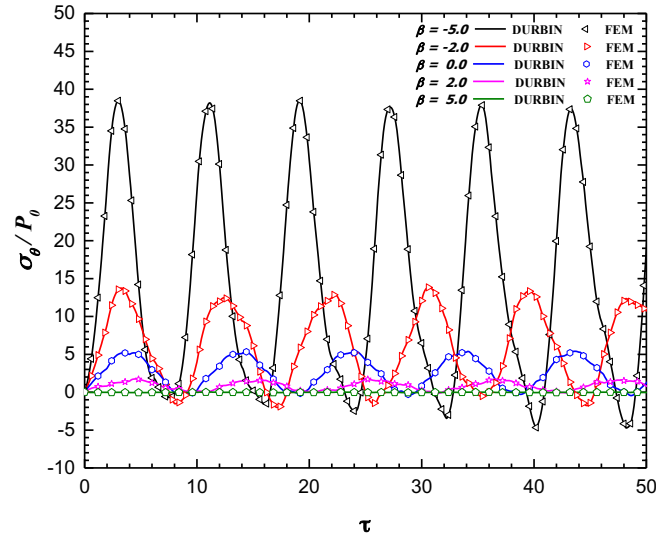


Fig. 3. Hoop stress versus time for rectangular impulsive load

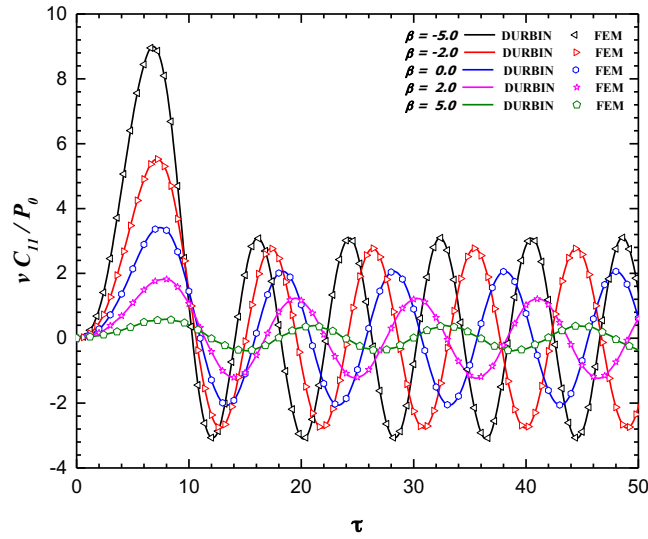


Fig. 4. Radial displacement versus time for triangular impulsive load

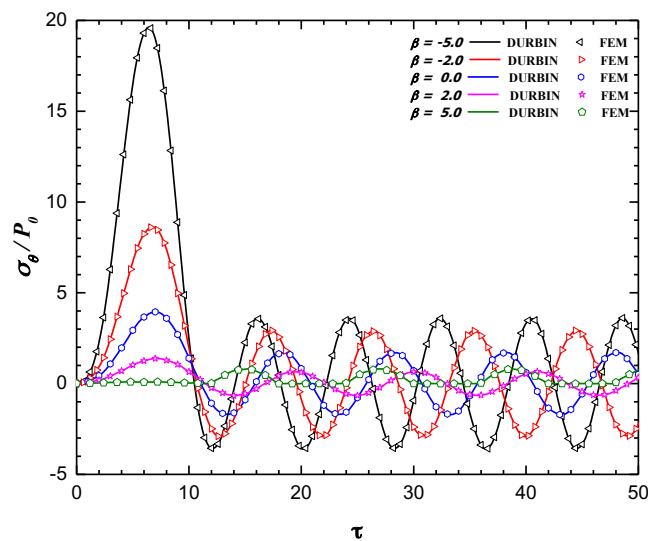


Fig. 5. Hoop stress versus time for triangular impulsive load

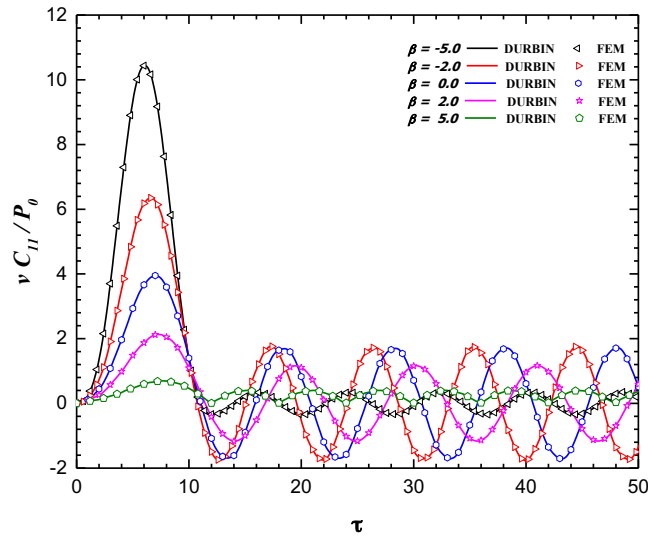


Fig. 6. Radial displacement versus time for half sinus impulsive load

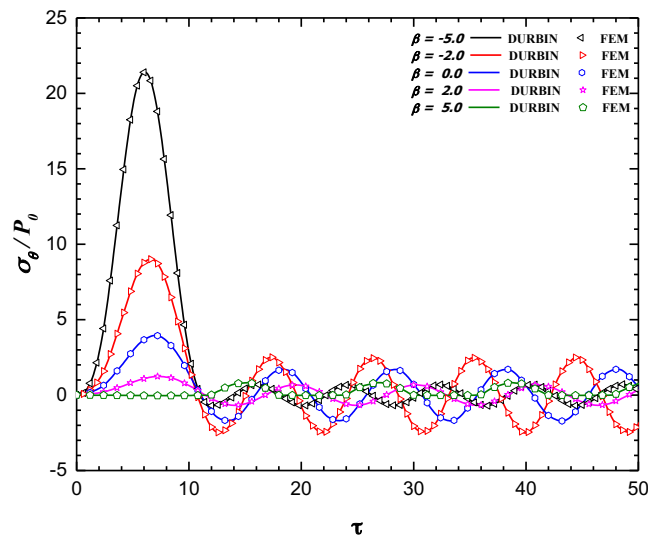


Fig. 7. Hoop stress versus time for half sinus impulsive load

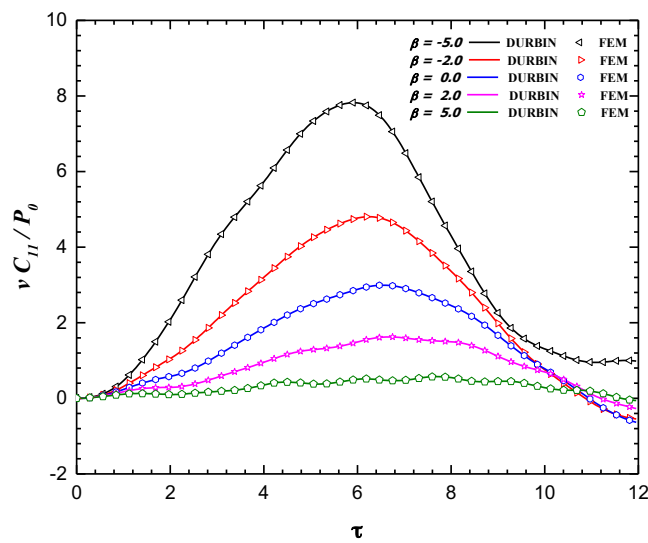


Fig. 8. Radial displacement versus time for impulsively load given discretely

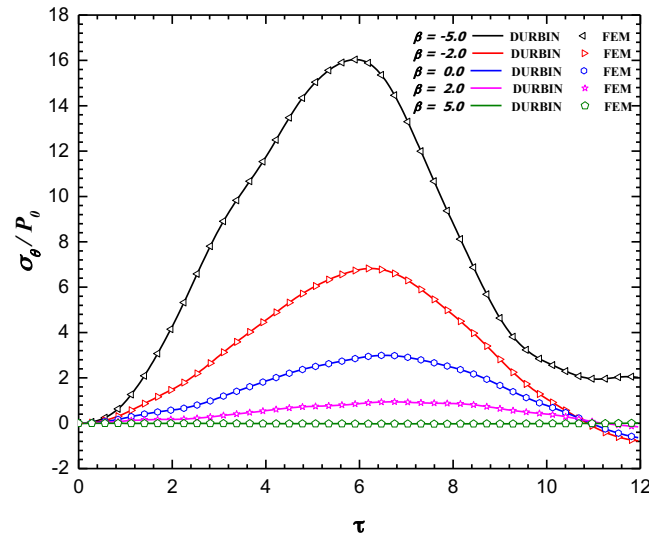


Fig. 9. Hoop stress versus time for impulsive load given discretely

6. Conclusion

Numerical model of FGM cylinders for stresses and displacement are obtained and solved by Durbin's method. The efficacy and adequacy of the present method is first compared to analytical results presented for constant Elastic Modulus and Poisson Ratio. The solution procedure can be applied to any continuous grading function option. The solution technique and procedure are simple, efficient and well structured, in addition to providing low cost accuracy. We have seen that FGM thick-walled cylindrical engineering structures with exponential variable properties have a significant effect on mechanical behavior. In particular, the positive inhomogeneity constant has a major effect on the stress distribution. Although the inhomogeneity parameter is a useful parameter in design, it can be applied for special applications in order to control stress distributions and displacement

References

- [1] Tranter, C., LXV. The application of the Laplace transformation to a problem on elastic vibrations. *The London, Edinburgh, and Dublin Philosophical Magazine and Journal of Science*, 33, 614-622, 1942
- [2] Mirsky, I., Axisymmetric vibrations of orthotropic cylinders. *The Journal of the Acoustical Society of America*, 36, 2106-2112, 1964
- [3] Klosner, J.M. and C.L. Dym, Axisymmetric, Plane- Strain Dynamic Response of a Thick Orthotropic Shell. *The Journal of the Acoustical Society of America*, 39, 1-7, 1966
- [4] Ahmed, N., Axisymmetric Plane- Strain Vibrations of a Thick- Layered Orthotropic Cylindrical Shell. *The Journal of the Acoustical Society of America*, 40, 1509-1516, 1966
- [5] Ghosh, A., Axisymmetric vibration of a long cylinder. *Journal of sound and vibration*, 186, 711-721, 1995
- [6] Güven, U.u., On stress distributions in functionally graded isotropic spheres subjected to internal pressure. *Mechanics Research Communications*, 3, 277-281, 2001
- [7] Tutuncu, N. and M. Ozturk, Exact solutions for stresses in functionally graded pressure vessels. *Composites Part B: Engineering*, 32, 683-686, 2001

- [8] Horgan, C. and A. Chan, The pressurized hollow cylinder or disk problem for functionally graded isotropic linearly elastic materials. *Journal of Elasticity*, 55, 43-59, 1999
- [9] Obata, Y. and N. Noda, Steady thermal stresses in a hollow circular cylinder and a hollow sphere of a functionally gradient material. *Journal of Thermal stresses*, 17, 471-487, 1994
- [10] Tutuncu, N. and B. Temel, A novel approach to stress analysis of pressurized FGM cylinders, disks and spheres. *Composite Structures*, 91, 385-390, 2009
- [11] Loy, C., K. Lam, and J. Reddy, Vibration of functionally graded cylindrical shells. *International Journal of Mechanical Sciences*, 41, 309-324, 1999
- [12] Pradhan, S., C. Loy, K. Lam, and J. Reddy, Vibration characteristics of functionally graded cylindrical shells under various boundary conditions. *Applied Acoustics*, 61, 111-129, 2000
- [13] Bayat, M., M. Saleem, B. Sahari, A. Hamouda, and E. Mahdi, Analysis of functionally graded rotating disks with variable thickness. *Mechanics Research Communications*, 35, 283-309, 2008
- [14] Xiang, H., Z. Shi, and T. Zhang, Elastic analyses of heterogeneous hollow cylinders. *Mechanics Research Communications*, 33, 681-691, 2006
- [15] Han, X., G. Liu, Z. Xi, and K. Lam, Transient waves in a functionally graded cylinder. *International Journal of Solids and Structures*, 38, 3021-3037, 2001
- [16] Shakeri, M., M. Akhlaghi, and S. Hoseini, Vibration and radial wave propagation velocity in functionally graded thick hollow cylinder. *Composite structures*, 76, 174-181, 2006
- [17] Ng, T., K. Lam, K. Liew, and J. Reddy, Dynamic stability analysis of functionally graded cylindrical shells under periodic axial loading. *International Journal of Solids and Structures*, 38, 1295-1309, 2001
- [18] Keles, I., *Elastic response of FGM and anisotropic thick-walled pressure vessels under dynamic internal pressure*. 2007, PhD thesis, Cukurova University.
- [19] Çalim, F.F., Dynamic analysis of beams on viscoelastic foundation. *European Journal of Mechanics-A/Solids*, 28, 469-476, 2009
- [20] Celebi, K., I. Keles, and N. Tutuncu, Closed-Form Solutions For Forced Vibration Analysis of Inhomogenous Rod. 2012
- [21] Celebi, K., I. Keles, and N. Tutuncu, Exact Solutions for Forced Vibration of Non-Uniform Rods by Laplace Transformation. *Gazi University Journal of Science*, 24, 347-353, 2011
- [22] Temel, B. and M.F. Şahan, Transient analysis of orthotropic, viscoelastic thick plates in the Laplace domain. *European Journal of Mechanics-A/Solids*, 37, 96-105, 2013
- [23] Liang, X., Y. Deng, Z. Cao, X. Jiang, T. Wang, Y. Ruan, and X. Zha, Three-dimensional dynamics of functionally graded piezoelectric cylindrical panels by a semi-analytical approach. *Composite Structures*, 226, 111176, 2019
- [24] Şahan, M.F., Viscoelastic damped response of cross-ply laminated shallow spherical shells subjected to various impulsive loads. *Mechanics of Time-Dependent Materials*, 21, 499-518, 2017
- [25] Wu, J.-S. and L.-K. Chiang, Out-of-plane responses of a circular curved Timoshenko beam due to a moving load. *International Journal of Solids and Structures*, 40, 7425-7448,

2003

[26] Daneshjou, K., M. Bakhtiari, and A. Tarkashvand, Wave propagation and transient response of a fluid-filled FGM cylinder with rigid core using the inverse Laplace transform. *European Journal of Mechanics-A/Solids*, 61, 420-432, 2017

[27] Watson, G.N., *A treatise on the theory of Bessel functions*. 1995: Cambridge university press.

[28] Durbin, F., Numerical inversion of Laplace transforms: an efficient improvement to Dubner and Abate's method. *The Computer Journal*, 17, 371-376, 1974

[29] Narayanan, G.V., *Numerical Operational Methods in Structural Dynamics*. 1981, PhD thesis, University of Minnesota.

[30] ANSYS Swanson Analysis System, Inc., 201 Johnson Road, Houston, PA 15342-1300, USA.,